Electrochemically Induced Dynamics of a Benzylic Amide [2]Catenane

Paola Ceroni,[†] David A. Leigh,*[,‡] Loïc Mottier,[†] Francesco Paolucci,*[,†] Sergio Roffia,[†] David Tetard,[‡] and Francesco Zerbetto*[,†]

Dipartimento di Chimica "G. Ciamician", Università degli Studi di Bologna, v. F. Selmi 2, 40126 Bologna, Italy, and Centre for Supramolecular and Macromolecular Chemistry, Department of Chemistry, University of Warwick, Coventry CV4 7AL, United Kingdom

Received: June 8, 1999; In Final Form: September 8, 1999

The electrochemistry of a benzylic amide [2]catenane was investigated and compared to that of its topologically trivial components. The redox behavior of both the catenane and the uninterlocked macrocycle can be largely understood in terms of the electrochemistry of smaller molecular fragments and simple molecular orbital considerations that show that the electroactivity of the C═O groups is split into two sets of quasi-degenerate potentials separated by a substantial gap. A fast intermolecular reaction follows the reduction of the macrocycle and smaller fragments, consistent with the corresponding dimers containing a new C−C bond linking two reduced carbonyls. The cyclic voltammetric behavior of the catenane differs significantly from that of the macrocycle—a feature that must therefore be directly attributable to the mechanically interlocked molecular architecture of the catenane. In particular, an intramolecular reaction (irreversible in the CV time scale) occurs in the catenane, which is shown to be a function of temperature and scan rate. Simulation of the cyclic voltammograms shows that the intramolecular reaction occurs on a time scale wider than that of circumrotation of the two rings in the neutral molecule, thus excluding that cyclic voltammetry (CV) is monitoring the latter process. Both the analysis of the electrochemical data and semiempirical quantum chemical (MNDO) calculations would suggest that the electrochemically induced reaction in the catenane is the soldering of the two interlocked macrocycles: the formation of a C−C bond between two reduced carbonyl groups would thus prevent further rotation of the two interlocked rings.

Introduction

The dynamic translational processes inherent in mechanically interlocked molecules (catenanes and rotaxanes) have understandably attracted considerable interest over the past few years because control over the kinetics and thermodynamics of how the individual components move with respect to each other is central to the development of nanoscale devices based upon such systems.[1−3] Hydrogen bond-mediated assembly offers a highly accessible route to such architectures, but the catenanes first prepared by such routes were based upon a hindered anilide system where, because of stringent steric requirements, the macrocyclic rings were restricted to rotating only a few degrees with respect to each other.[4] In contrast, benzylic amide catenanes display a rich variety of dynamic behavior in terms of macrocyclic ring circumrotation;[5] variations in solvent polarity and structural changes in the catenanes allow the frequency of circumrotation of this class of compounds to be varied over at least 9 orders of magnitude! Recently,[6] electrochemistry has been used to moderate molecular recognition processes based upon hydrogen bonding—the principal[5] mode of interaction between the rings in benzylic amide catenanes and a major factor in determining the rates of macrocycle circumrotation. It was therefore of interest to investigate the cyclic voltammetric behavior of the [2]catenane **1** to see if it could be understood in terms of the behavior of its noninterlocked components.

In general, two fundamental sets of information can be acquired from CV studies: knowledge of the energy location of redox orbitals involved in the heterogeneous charge-transfer processes and data concerning the dynamics and/or reactivity proper to the oxidized/reduced forms of molecules. In the case in question, comparison of the results obtained for the catenane and its building blocks outlines a picture where unique electrochemical properties are found to be intrinsic to the catenane. The structural complexity of the system under investigation required that the experimental work be accompanied by a computational analysis that consists of the simulations of the CV curves and a quantum chemical approach to the molecule itself. This dual approach establishes a special role in the electrochemistry played by the mechanically interlocked architecture.

Experimental Section

Synthetic Procedure. The benzylic amide [2]catenane **1** and macrocycles **2** and **2′** were synthesized and isolated according to literature procedures.[1e,h] Fragments **3** and **4** were prepared from the condensation of the corresponding commercially available amines and acid chlorides and purified by column chromatography on silica gel (93 and 95% yields, respectively).

Electrochemical Experiments. All materials were reagent grade chemicals. Tetraethylammonium tetrafluoroborate (TEATFB, puriss from Fluka), was used as supporting electrolyte as received. DMF (UVASOL, Merck) or THF (LiChrosolv, Merck) was distilled into the electrochemical cell, prior to use, using a trap-to-trap procedure. The purification procedures relative to DMF and THF have previously been described.[7b,c]

* Corresponding authors. E-mail addresses: David.Leigh@Warwick.ac.uk, paolucci@ciam.unibo.it, gatto@ciam.unibo.it.
[†] Università degli Studi di Bologna.
[‡] University of Warwick.

10.1021/jp991870+ CCC: $18.00
Published on Web 11/03/1999

In some curves a small peak, at ca. −2.0 V, is observed, which is due to residual anthracene present in the purified DMF.

The single-compartment electrochemical cell was of airtight design with high-vacuum glass stopcocks fitted with either Teflon or Kalrez (DuPont) O-rings to prevent contamination by grease. Connections to the high-vacuum line and to the Schlenck tube containing the solvent were provided by spherical joints also fitted with Kalrez O-rings. The pressure measured in the electrochemical cell prior to trap-to-trap distillation of the solvent was typically 1.0×10^{-5} to 2.0×10^{-5} mbar. The working electrode consisted either of a 0.6 mm diameter platinum wire (electroactive area ~0.15 cm^2) or a Pt disk ultramicroelectrode ($r = 5\ \mu m$), both sealed in glass. The counter electrode consisted of a platinum spiral, and the quasi-reference electrode was a silver spiral. The quasi-reference electrode drift was negligible for the time required for a single experiment. Both the counter and reference electrodes were separated from the working electrode by ~0.5 cm. Potentials were measured with a ferrocene standard and referenced to SCE.[7] $E_{1/2}$ values correspond to $(E_{pc} + E_{pa})/2$ from CV. In some experiments a SCE reference electrode was used, separated from the working electrode compartment by a sintered glass frit. Ferrocene was also used as an internal standard for checking the electrochemical reversibility of a redox couple. The number of electrons corresponding to an electrochemical process was determined by comparison to ferrocene used as an internal standard and, independently, from the value of the limiting current ($i_{lim} = 4nFDcr$) at a disk ultramicroelectrode (with radius $r = 12.5\ \mu m$ and concentration of the electroactive species c), according to a procedure described elsewhere.[8]

Potential-controlled bulk electrolysis was carried out in a three-compartment electrochemical cell with both the SCE reference electrode and the platinum spiral counter electrode separated from the working electrode compartment by sintered glass frits. The working electrode was a large area platinum gauze. The electrolized solution was monitored at intervals during the electrolysis by steady-state voltammetry, and at the same time, UV−vis spectra were taken.

The temperature dependence of the ferrocenium/ferrocene couple standard potential was measured with respect to SCE by a nonisothermal arrangement according to a method outlined in the literature.[9]

Voltammograms were recorded with a AMEL model 552 potentiostat or a custom made fast potentiostat[10] controlled by either an AMEL model 568 function generator or an ELCHEMA model FG-206F. Data acquisition was performed by a Nicolet Mod 3091 digital oscilloscope interfaced to a PC. The charge exchanged during bulk electrolysis was measured by a AMEL model 731 digital integrator. UV−vis spectra were taken using a VARIAN Cary 5E UV−vis−NIR spectrophotometer. Temperature control was accomplished within 0.1 °C with a Lauda Klein-Kryomat thermostat.

Digital Simulation of Cyclic Voltammetric Experiments. The CV simulations were carried out by either the DigiSim 2.1 software by Bioanalytical Systems Inc. or the program Antigona developed by one of us (L.M.). All the electrochemical steps were considered fast in the simulation, and the chemical rate constants were chosen so as to obtain a visual best fit over a 10^2-10^3-fold range of scan rates.

Results and Discussion

The present CV investigation focuses on the properties of the anions of benzylic amide [2]catenane **1** and their comparison with those of its building blocks, macrocycle **2** and fragments **3** and **4** (Figure 1). As a first step, we consider then a qualitative analysis of the molecular orbitals (MO's) that are filled during the electrochemical experiments.

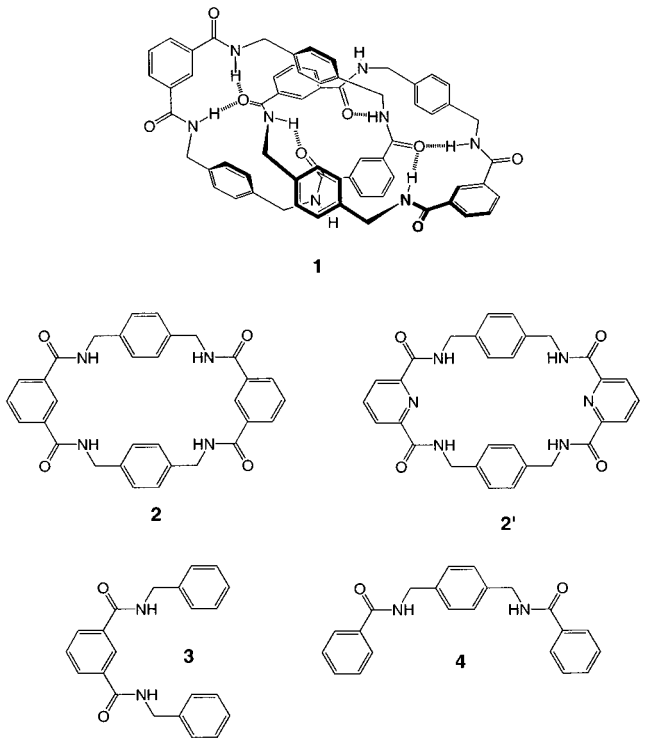

Figure 1. Benzylic amide catenane **1**, its parent macrocycle **2**, the pyridine-analogue macrocycle **2′**, and fragments with (a) two conjugated carbonyls (**3**) and (b) two nonconjugated carbonyls (**4**).

Building Up the Molecular Orbitals. In the benzylic amide catenane **1**, two different types of centers with low lying unoccupied orbitals are present: the first are the xylylene rings (para-substituted phenyl groups), the second are the isophthaloyl groups (meta-substituted phenyl rings conjugated to two carbonyl groups). The molecular orbitals of benzene have long been a textbook example;[11] in particular, the LUMO is doubly degenerate and its electron affinity is 1.12 eV. As for the carbonyl group, in formaldehyde the antibonding π^* orbital has an electron affinity of 0.86 eV. Since the combination of the phenyl and the carbonyl groups will decrease the energy of π_{CO}^*, effectively, this makes (in a hypothetical benzaldehyde fragment) π_{CO}^* the first MO available to electrons in a reductive CV experiment.

On the way toward building a qualitative understanding of the unoccupied MO's of the catenane, the next two effects to consider are (i) the influence of the NH group and (ii) the consequence of having *two* amide groups in the meta positions of the isophthaloyl fragment. The amido nitrogen behaves as an electron donor whose activity is due to the n_N orbital. As such, it interacts mainly with the n_O and should not significantly affect the energy of π_{CO}^*. Addition of a second amide substituent can be treated at various levels of sophistication. In the simplest approach, and in analogy to what was done above for the interaction between the π^* orbitals of the phenyl and the carbonyl groups, one can consider a two-level system. This is formed by the two π_{CO}^* groups individually perturbed by the phenyl orbitals that are allowed to further interact with one another via the phenyl group. Owing to the conjugation, the amount of interaction is sizable and one can expect that the plus combination of the two perturbed π_{CO}^* orbitals will be substantially shifted with respect to its minus counterpart.

To extend the present approach to the macrocycle, one can take a different fragment in which the methylene groups of the *p*-xylylene rings are each substituted by −NH−CO− groups. The discussion given above can be reapplied with slight modifications. Both interactions will now be weaker for lack of conjugation, and one can therefore expect a reduction potential in which the two carbonyls are reduced roughly at the same potential. The small energy gap between the two reductions that may or may not be observed is then due to hyperconjugative effects, i.e., through-bond and through-space interactions. Application of the model to the four π_{CO}* orbitals of the macrocycle yields two pairs of quasi-degenerate orbitals separated by a sizable gap. Apart from Coulombic effects, the macrocycle should therefore have two quasi-degenerate lower lying reduction potentials followed at higher potentials by two more quasi-degenerate ones. In the same spirit, extrapolating to the catenane would only double the value of the number of reducing electrons. Complications can, however, arise because of the possibility of localization or delocalization of the fragment orbitals and of the possible presence of dynamics.

Are the Fragment Molecular Orbitals Delocalized in the Catenane? To investigate further the nature of the electronic wave function of anionic states, two extreme possibilities can be envisaged: in the first, the reducing electrons are strongly delocalized over the entire molecule; in the second, they are totally localized on a particular carbonyl group.

The delocalized picture can be approached in the high-symmetry regime. In this case, the catenane can ideally be represented by two perpendicular interlocked rectangles. Notice that this does not require the macrocycles to be planar; rather, it simply necessitates that each macrocycle has the symmetry of a rectangle, namely, D_{2h} symmetry. With this prescription, the catenane has D_{2d} symmetry, a group that is nonabelian and admits a degenerate representation. We emphasize that in the solid,[1e] and probably in solution as well, the molecular symmetry is actually much lower. In D_{2d} symmetry, eight local orbitals that do not fall on a symmetry element, transform as $A_1 + A_2 + B_1 + B_2 + 2E$. If four of them fall on the principal axis; they transform as $2A_1 + 2B_1 + 6E$. Although we have started in a picture in which the MO's and therefore the charge(s) of the anion(s) are local, group theory furnishes a simple way to delocalize them over the entire molecule. The present treatment is implicit in the perturbation theory of degenerate levels that, however, cannot provide (without a direct calculation) the coefficients that describe the delocalization. Such coefficients are simple to obtain in group theory.

The conclusion is that both symmetry (and perturbation theory of degenerate levels) delocalize the MO's and therefore the charge(s). Notice that environmental effects that single out individual fragments and thereby lift the degeneracy can, on the contrary, effectively localize it (them).

Voltammetric Behavior. In building up a strategy toward the comprehension of the electrochemical properties of the benzylic amide catenane **1**, a bottom-up approach was adopted in which macrocycle **2** (and **2′**), and the two fragments **3** and **4** depicted in Figure 1, are first considered before passing to catenane **1**.

The CV curve for a 1.0 mM **2** DMF solution, at 25 °C and $\upsilon = 1$ V s^{-1} (Figure 2a), shows a single, two-electron, irreversible peak. The effect of either scan rate increase (Figures 2b) or temperature decrease (Figure 2c) on the CV morphology proved the chemical nature of such irreversibility. The number of electrons corresponding to the reduction peak was determined by comparison to ferrocene used as an internal standard and,

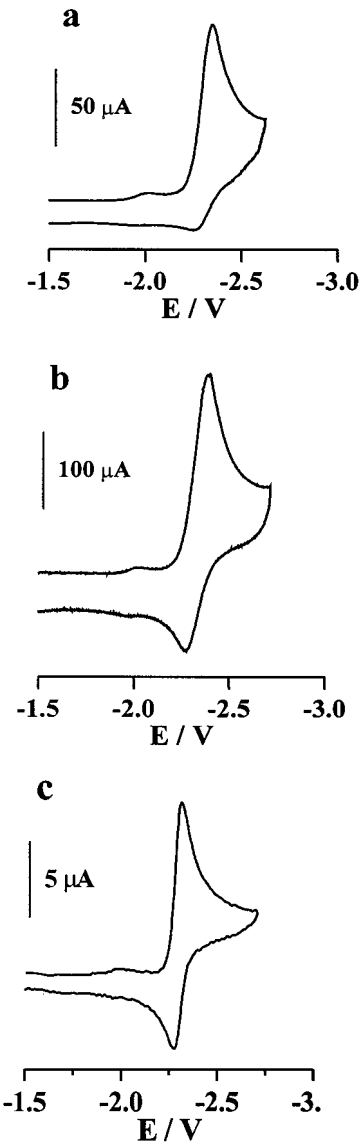

Figure 2. CV curves of **2**, 1.0 mM in DMF, 0.05 M TEATFB: (a) $T = 25$ °C, $\upsilon = 1$ V s^{-1}; (b) $T = 25$ °C; $\upsilon = 10$ V s^{-1}; (c) $T = -54$ °C; $\upsilon = 0.2$ V s^{-1}. Working electrode: Pt.

independently, by the method described in the Experimental Section. The two-electron peak becomes fully reversible at $\upsilon \geq 100$ V s^{-1} (25 °C) with an apparent $E_{1/2}$ value of −2.31 V. The simulation of the CV curves (vide infra) finally yielded the $E_{1/2}$ values for the corresponding one-electron processes, which are −2.29 and −2.33 V, respectively. The 0.04 V difference between the two processes is that expected for two equivalent noninteracting redox sites[12] which, based on the qualitative description of the MO's given above, are located each on one isophthaloyl group in **2**. At 25 °C and scan rates below 2 V s^{-1}, a second cathodic peak (II) is observed within the available potential window (Figure 3a), which, however, corresponds to a much lower charge than that of I. Such a peak was not observed in the background curve and proved therefore to be due to some product of the chemical reaction coupled to reductions I. At −54 °C, peak II is not observed, while, within the enlarged available potential window, another cathodic peak (III) appears, with $E_p = -2.93$ V (Figure 3b). Comparison to peak I, also by means of convolutive analysis of the CV curve,[13] showed that peak III corresponds to the exchange of one electron. It is not reversible, while an anodic, ill-defined peak occurs, in the reverse scan, at around −2.6 V. Furthermore, the

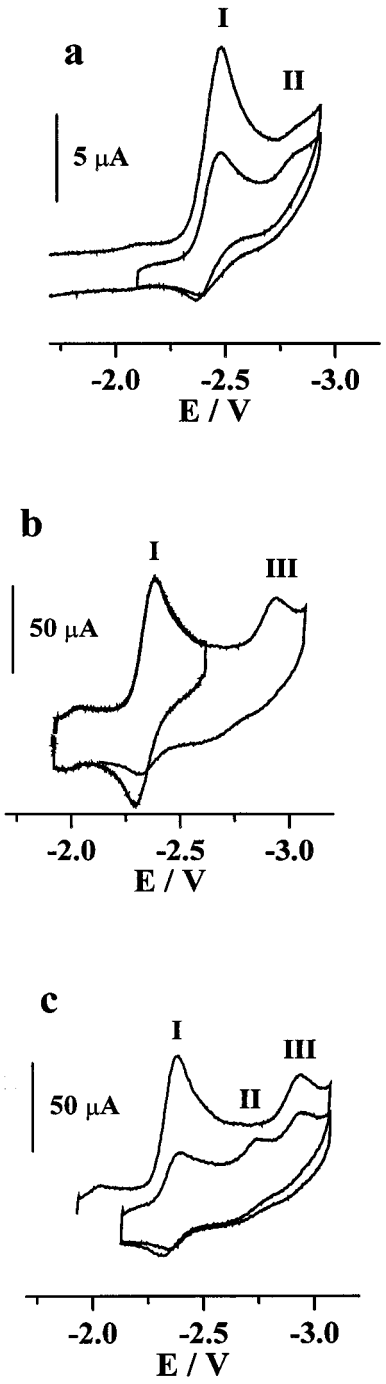

Figure 3. (a) CV curve of **2**, 1 mM in DMF, 0.05 M TEATFB, T = 25 °C, v = 1 V s^{-1}; (b) partial and global CV scan of **2**, 1 mM in DMF, 0.05 M TEATFB, T = -54 °C, v = 5 V s^{-1}; (c) multiple scan CV curve of **2**, 1 mM in DMF, 0.05 M TEATFB, T = -54 °C, v = 5 V s^{-1}. Working electrode: Pt.

occurrence of peak III reduction strongly affects the reversibility of peak I (Figure 3b). The two-scan curve in Figure 3c shows, during the second scan, a very large decrease of peak I and, at the same time, the reappearance of peak II. The anodic peak at −2.6 V may represent the anodic partner of peak II; one can therefore gather that the same chemical reaction coupled, at high temperatures and low scan rates, with reduction I, follows, at low temperatures and high scan rates, reduction III. Finally, peak III corresponds to the further reduction of pristine (doubly reduced) **2**, and the potential separation between peaks I and III is therefore a measure of the coupling interaction of two electrons added in the same isophthaloyl group.

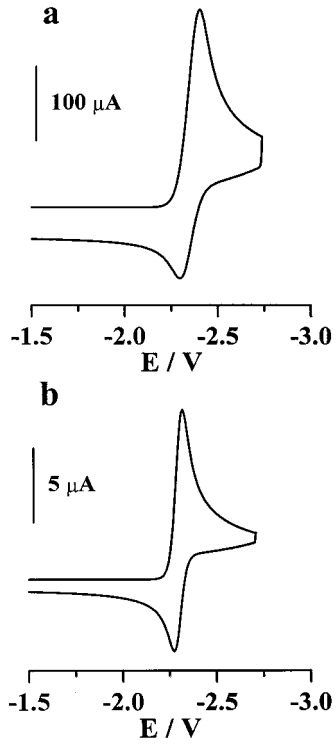

Figure 4. (a), (b) Simulated CV curves for the first reduction of macrocycle **2** under the conditions of Figure 2b,c, respectively, calculated according to the dimerization mechanism decribed in the text.

Notable, in the CV curves shown in Figure 3a,c, is the large decrease of peak current during the second scan, much larger than that expected for diffusional loss. Furthermore, concentration effects on the CV morphology were clearly observed. Both the decrease of peak I height during the second (and successive) scans and its irreversibility, at a given scan rate, become increasingly less important with diminishing macrocycle concentration. The occurrence of a second-order reaction dimerization following the two-electron reduction I was checked by performing the digital simulation of the CV curves. The simulation was performed over a 3-order-of-magnitude scan rate range and with the **2** concentration ranging from 2.0 to 0.2 mM. In Figure 4a,b, the simulated curves calculated under the conditions of Figure 2b,c respectively are shown, exemplifying the very good agreement between simulated and experimental curves generally obtained under the various conditions. From simulation, the following kinetic parameters relative to the dimerization reaction were obtained: $k_{25°C}$ = 60 000 M^{-1} s^{-1}; $k_{-54°C}$ = 450 M^{-1} s^{-1}, and E_a = 8.03 kcal mol^{-1}. In line with this result, peak II therefore represents the reduction of the dimeric species. A possible explanation for the much lower current observed for such a peak compared to peak I is therefore the fact that only one electron would be exchanged and that the concentration of electroactive species would be halved by the dimerization process.

Not surprisingly, a very similar CV behavior to that of **2** was observed for fragments **3** and **4**. These are expected to be complementary models for understanding the redox properties of **2**, since they contain either conjugated or nonconjugated benzylic amide groups. The CV curves obtained at 25 °C and 1 V s^{-1} for 0.5 mM DMF solution of **3** and **4** are shown in Figure 5a,b, respectively. Under these conditions, irreversible CV patterns are observed. In both cases, reversibility was attained by either increasing the scan rate or decreasing the temperature. The reduced conjugated fragment **3** was found to

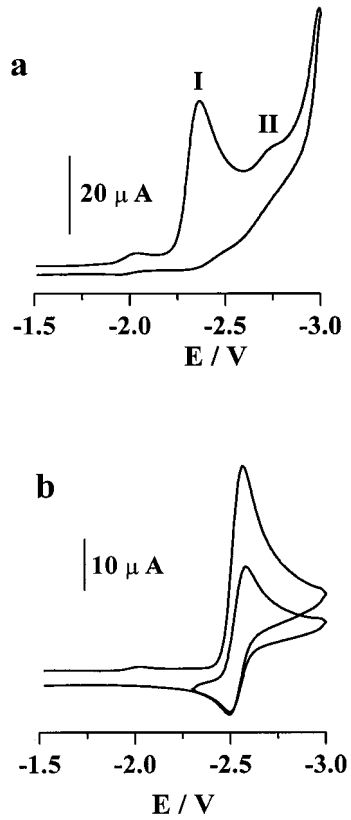

Figure 5. CV curves of (a) **3** and (b) **4**: 0.5 mM in DMF, 0.05 M TEATFB, $T = 25$ °C, $\upsilon = 1$ V s^{-1}. Working electrode: Pt.

be more reactive than the nonconjugated one **4**: at 25 °C, full reversibility was obtained for **3** at $\upsilon \geq 200$ V s^{-1} and for **4** at $\upsilon \geq 100$ V s^{-1}. The $E_{1/2}$ values measured under these conditions are -2.34 and -2.54 V, respectively. Moreover, the reduction peak corresponds to a one-electron process in **3** and to a two-electron one in **4**. This is expected on the basis of the location of redox orbitals given above, since little interaction is expected to occur between amide groups in **4**. On the other hand, the lack of the second amide group in the meta position increases the energy of the redox orbitals, explaining why these reductions are shifted cathodically in **4** with respect to the corresponding processes in **2**. Finally, concentration changes were also found to affect the CV morphology of the two fragments and the simulation of the CV curves substantiated the hypothesis that the same dimerization mechanism observed in the case of **2** is operating here. The different reactivity found for reduced **3** and **4** may be explained in terms of a different electrostatic repulsion between reduced fragments, higher as expected in the case of **4** (dianion) than in **3** (monoanion).

A notable difference between the CV curves of the two fragments is that only in the case of conjugated species **3** may a further peak having the characteristics of peak II in **2** be observed (Figure 5a). This identifies such a peak as due to a product of the irreversible reduction of the species containing at least two conjugated carbonyls. In light of the proposed location of redox processes, the addition of an electron forms, in all the species considered, a radical anion at one of the carbonyls with the negative charge largely localized on the oxygen and the radical center at the carbon. A known possible fate of reduced aromatic amides[14] is the rupture of the C−N bond. However, fragmentation was proved not to occur to any significant extent by bulk electrolysis experiments (vide infra). A possible reaction involving the reduced carbonyls, also compatible with the results of digital simulation of the CV

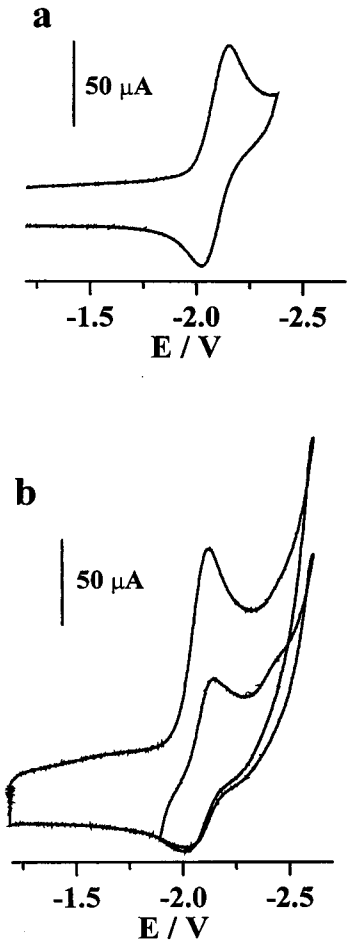

Figure 6. CV curves of **2′**, 1 mM in DMF, 0.05 M TEATFB, $T = 25$ °C, $\upsilon = 1$ V s^{-1}.

curves, is a coupling reaction forming a bond between two carbonyls belonging to different molecules. The resulting species is not expected to be highly stable, but further stabilization might come from coupled reactions such as, for instance, protonation. This would explain the irreversibility of such a reaction on the CV time scale: the carbonyls involved in the coupling would be no longer able to exchange electrons at the electrode, thus explaining the observed large decrease of peak currents. At the same time the coupling reaction breaks the conjugation between the two carbonyls in the same isophthaloyl group and peak II might then correspond to the following reduction of the residual carbonyl.

Also in line with this hypothesis is the result of the CV investigation on the pyridine analogue of **2**, species **2′** in Figure 1. The same CV behavior as in **2** is observed with two notable differences: (i) the first peak, which again corresponds to two electrons, is already reversible at $\upsilon = 1$ V s^{-1} ($T = 25$ °C, Figure 6a); (ii) the corresponding $E_{1/2}$ value is shifted anodically with respect to **2** by 240 mV ($E_{1/2} = -2.07$ V). While such an anodic shift may be easily interpreted in terms of the higher electronegativity of pyridine with respect to benzene, the hindering of the dimerization reaction has to be attributed, in the absence of either steric or charge differences between the two macrocycles, to a greater delocalization of the unpaired electron over the aromatic ring. This would make reduced carbonyl clearly less reactive. Figure 6b shows that, on extending the scan to the cathodic limit, under the conditions of Figure 6a, affects the reversibility of peak I during the reverse scan. Moreover, a second scan reveals morphological changes very similar to those observed in **2** (cf. Figure 3a).

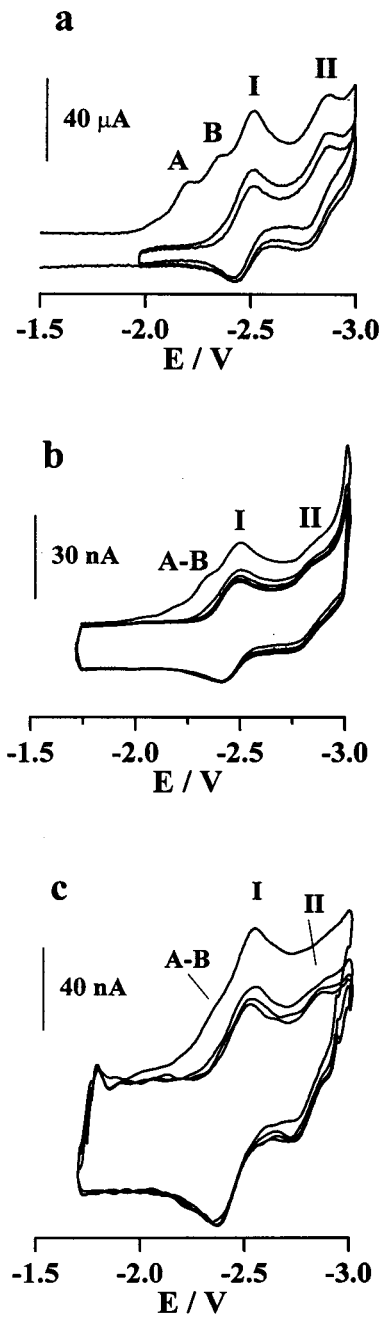

Figure 7. CV curves of **1**, 0.5 mM in DMF, 0.05 M TEATFB, $T = 25$ °C: (a) $\upsilon = 10$ V s^{-1}; (b) 500 V s^{-1}; (c) 7000 V s^{-1}. Working electrode: Pt. For (b) and (c) a disk Pt ultramicroelectrode, $r = 5$ μm, was used.

The dynamics of the catenane reduction is far more complicated than that of the parent macrocycle. Figure 7 shows the CV curves of a 0.5 mM **1** DMF solution, obtained under various conditions. Two major peaks, as observed in the CV of **2** (I and II), are present at low scan rates and room temperature (Figure 7a). At variance with **2**, however, peak I has developed two side peaks at less negative potentials. For simplicity they can be called A and B, appearing as shoulders in the rising part of peak I. Proper peak I is roughly twice the height of peaks A and B (for the determination of the number of electrons see the Experimental Section). Peaks A and B are irreversible under the conditions of Figure 7a-b, lacking their anodic partners even when the scan is reversed right after the peaks themselves. As scan rate is increased peak A shifts cathodically toward B eventually coalescing into a single peak ($\upsilon \geq 2000$ V s^{-1}),

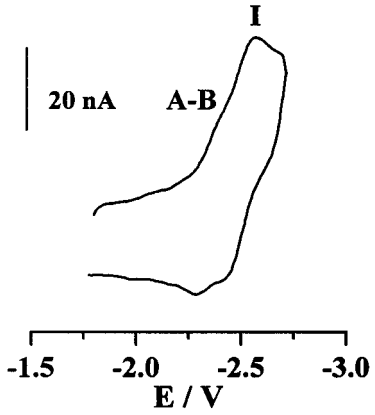

Figure 8. CV curve of **1**, 0.5 mM in DMF, 0.05 M TEATFB, (a) $T = 25$ °C; $\upsilon = 2000$ V s^{-1}. Working electrode: disk Pt ultramicroelectrode, $r = 5$ μm.

SCHEME 1: Electrochemical Reduction of Catenane 1

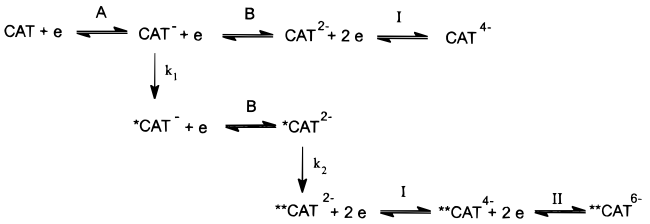

together appearing as a shoulder very close to peak I. Under these conditions, anodic partners of both peaks A−B and I are observed when the scan is reversed right after peak I, although full reversibility was not reached for the former two peaks, Figure 8. Parallely, peak II is smeared out (see Figure 7c, $\upsilon = 7000$ V s^{-1}). Importantly, however, II reappears in the reverse scan and in the successive curves obtained without the renewal of the diffusion layer. Decreasing the temperature does not modify the trend but modifications of the CV pattern evolve within a narrower scan rate range.

On the basis of the heights of the peaks, also compared to those for **2**, **3** and **4**, the overall first process corresponds to the transfer of four electrons with A, B, and proper I uptaking one, one and two electrons each. Under conditions which minimize the effect of chemical reactions coupled to electron transfers, the first two and the second two reductions can be arranged into two doublets of nearly degenerate processes. At lower scan rates, the first two reductions, and in particular A, are shifted to less negative potentials, as an effect of fast reactions occurring after the electron injections. By contrast, peak I is both electrochemically and chemically reversible. Peak II is instead due to the product of the reaction(s) involving the species produced by the first two reductions. At high scan rates, peak II is observed only during the second scan. This behavior is reminiscent of that of **2**. In contrast to that, however, no clear concentration dependence of the CV pattern was observed in **1**. Finally, the equivalent of peak III of **2** is not visible in the curves and is likely to occur just beyond the cathodic limit. The molecular orbital picture can explain such higher potential values in terms of a larger interaction present in **1,** which pushes the second set of four levels to values of the potential higher in **1** than in **2**. A reaction scheme outlining the described CV behavior of **1** is shown in Scheme 1.

A similar reactivity of reduced carbonyls in **1** as in **2**−**4** is expected. However, since no concentration dependence is observed in the case of **1**, the difference between them, which may in fact explain the unique features of the CV behavior of

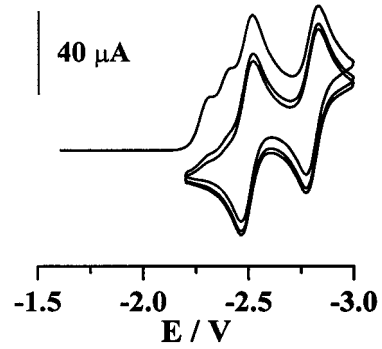

Figure 9. Simulated CV curve of **1**, under the conditions of Figure 7a, calculated according to the mechanism of Scheme 1.

the catenane, is that *the formation of an intramolecular bond between two reduced carbonyls belonging to different macrocycles* may in this case occur. The simulations of the CV curves were performed on the basis of the hypothesis that (i) the four redox processes forming the first peak are grouped into two closely spaced doublets centered around an $E_{1/2}$ value close to those for the two equivalent reductions in **2** (−2.42, −2.44, −2.46, and −2.49 V) and (ii) two different first-order reactions are coupled to the first two of the four reductions. In Figure 9, the CV curve, simulated according to the mechanism outlined in Scheme 1, and under the conditions of Figure 7a, is shown. The agreement with the experimental curve is rather good. The values for the rate constants k_1 and k_2, provided by the simulations, were respectively 5×10^5 s^{-1} and 4×10^3 s^{-1} (at 25 °C). By simulating curves obtained at different temperatures in the range +25 to −54 °C the following activation energies were obtained for the two processes involving CAT^- and $*CAT^{2-}$ respectively: 9 and 1 kcal mol^{-1}.[15] It is worth mentioning that at least the first process monitored electrochemically is very similar to the circumrotation of the two macrocycles of the catenane in polar solvents.[5] In CD_3OD, for instance, $\Delta G^{\ddagger}_{298} = 11.3$ kcal mol^{-1}. Reduction of one or more carbonyls however should *increase* the ability of the molecule to form intramolecular hydrogen bonds, increasing therefore the barrier and slowing down the circumrotation. Proof that the electrochemistry is not monitoring the circumrotation is in the facile presence of irreversibility in the processes discussed above. For the same reasons, the intramolecular proton transfer between an amide group in one ring and the reduced carbonyl in the other might in fact occur, coupled to the first reduction process (Scheme 2). Such a reaction could be irreversible on the time scale of CV. Protonation would also finally assist the coupling reaction between carbonyls occurring after the injection of the second electron (peak B), which results from the simulation being almost barrierless.

Attempted Isolation of the Electrochemical Products. The electrochemical work has so far shown several interesting features of the MO's and the dynamics of the catenane and its building blocks. Cyclic voltammetry can positively identify the products that are formed only by comparison of an authentic sample of the reaction product, but it can, nonetheless, narrow them down to a few possibilities. The results of the CV study are summarized as follows: the notable lowering of the heights of the peaks in the scans without renewal of the diffusion layer indicates that the dimerization reaction (concentration-dependent intermolecular reaction in **2**, **2′**, **3**, and **4** or intramolecular coupling in **1**) involves two electroactive groups that are therefore *lost* in the CV time scale. This is confirmed by the digital simulation of the CV curves. At the same time, the appearance of peak II within the gap between the successive reductions of conjugated carbonyls, substantiates the hypothesis that the reaction strongly affects the energetics of the remaining carbonyls, making them more easy to reduce, an effect compatible with either conjugation removal or proton transfer to reduced carbonyls.

To obtain information about the product, a 1.0 mM DMF solution of **1** was electrolyzed at −2.60 V. As the electrolysis proceeded, two absorption bands centered at 310 and 470 nm developed. At the end of the quantitative four-electron reduction of **1** (110% of the theoretical charge) the solution was a deep yellow. Reoxidation rapidly turned it to a pale yellow, a color that is, however, also present in the product of electrolysis (at the same potential) of a DMF solution containing only the supporting electrolyte. Similar experiments were also performed in **1**−THF solutions, where the same spectral changes were obtained. ^{1}H NMR analysis of the electrolysis product of **1** (after reoxidation) showed only the presence of the original catenane, indicating that the *product of the intramolecular reaction is highly labile in its neutral state*. The same (negative) result was obtained with macrocycle **2**. Finally, attempts to stabilize the product of electrolysis by methylation (by adding CH_3I either at the beginning or at the end of electrolysis) or by protonation (H_2O) also failed to give any isolable species other than the starting compound. As a contribution toward a more detailed comprehension of the proposed reactivity of the carbonyls, one can perform semiempirical quantum chemical calculations of the MNDO type. Any quantum chemical calculation requires the knowledge of the molecular connectivity. Such connectivity is most evident for the neutral system but it must be surmised in the case of the dianion. It was therefore decided to investigate the soldered structure proposed above. As a first step, it was necessary to verify if the newly formed dianion is stable. Geometry optimization of the doubly charged catenane resulted in a minimum in which the C−C bond distance is 1.701 Å. This is a rather long bond whose length is somewhere between the length of the strained C−C bond such as that of [1.1.1]-propellane in the ground state, 1.61 Å, and the length of the same bond in the first triplet excited state, 1.82 Å, where it is believed to be severed.[16] Step by step elongation of the bond afforded the construction of the dissociation curve whose activation barrier was found to be 8.3 kcal/mol. This value could be compared with that of the dimerization of two RC_{60} radicals, which are in the range 17.0−35.5 kcal mol^{-1}.[17] Perhaps unsurprisingly, the dissociated system in the vacuum is calculated to be more stable by 27.1 kcal mol^{-1} than the dianion in which the carbons are coupled. This partial picture appears to indicate that the proposed reactivity is at least plausible, although the lower energy of the reagent, at least in the vacuum, does pose a problem. Further support for the model came unexpectedly from the attempt to optimize the neutral species, which spontaneously rearranged to the original catenane. Implicitly, this can explain the inability to isolate anything but the original catenane despite unambiguous evidence for an irreversible (under the CV conditions and time scale) intramolecular reaction. The tentative conclusion that one can derive from the calculations is that soldering can take place as envisaged in Scheme 2, although, in all likelihood, other processes, such as protonation not included in the model, may intervene to stabilize the product.

Summarizing, the evidence provided from the electrochemical study and from theoretical considerations build up a picture of reductive behavior of **1** in which a major role is played by the amide carbonyl groups. The presence of an extra electron in the catenane forms a radical anion at one of the carbonyls with

SCHEME 2: Mechanistic Account for the CV Behavior of 1

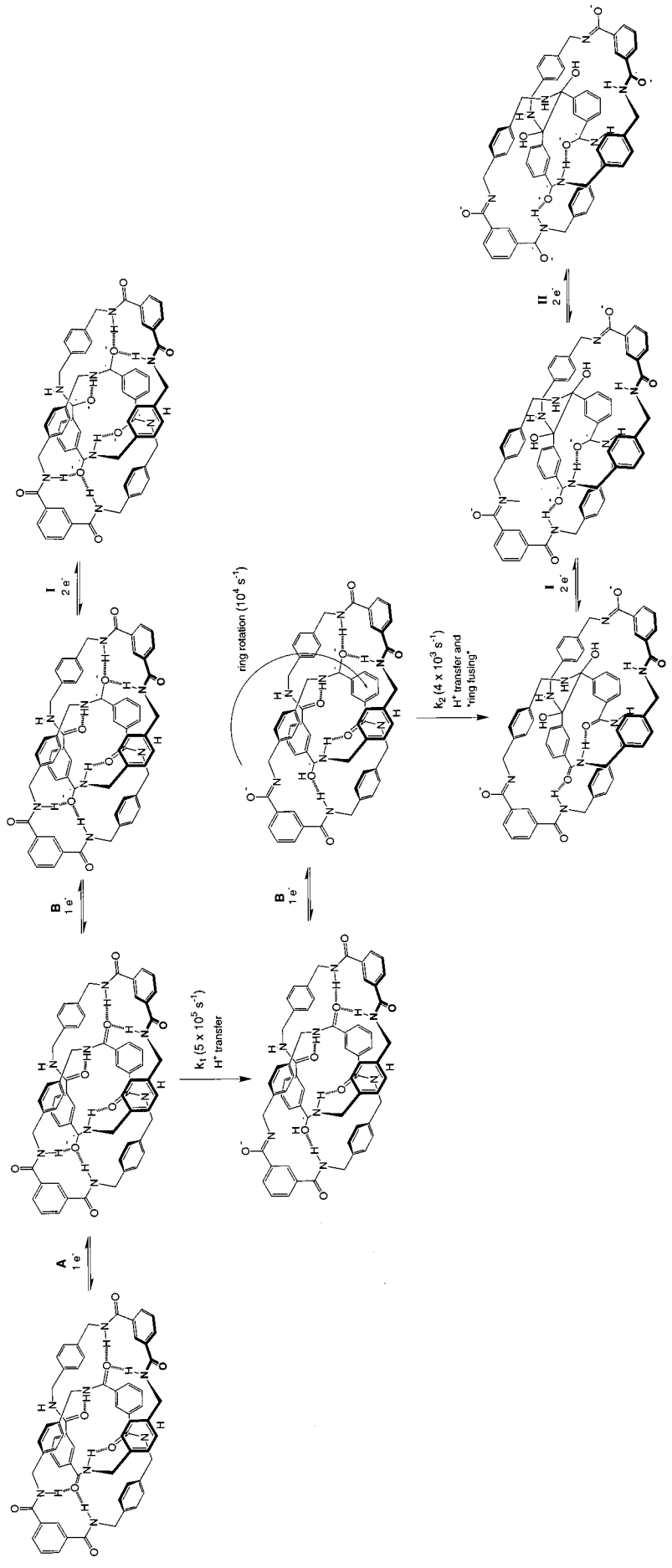

the negative charge largely localized on the oxygen and the radical center at the carbon. Addition of the second electron creates a second center with the same characteristics of the first. Both the electron transfers are complicated by fast kinetics involving the radical anions. The absence of concentration effects on the CV pattern, the fact that two electrons are lost in peak I in the second scan CV curve, and the appearance of a new two-electron reduction peak in the CV curve (peak II) at more negative potentials point toward a reaction product whose possible structure contains a covalent bond between the carbon atoms of carbonyl groups from the two macrocycles. Such a structure would arise from coupling of the radicals formed by the reduction of carbonyls on different rings brought into close proximity by macrocyclic ring rotation of the catenane. Of course, soldering together the two catenane rings through a covalent bond would prevent further rotation of either ring, electrochemically braking of the circumrotation process.

Conclusion

The electrochemistry of the benzylic amide catenane **1** derives directly from that of its parent macrocycle **2**, which in turn can be understood in terms of the simpler fragments **3** and **4** and pyridine analogue **2′**. It develops, however, in richer forms than its topologically trivial components in its CV curve at the level of the first set of carbonyl reductions. The grouping of the four reductions involving four equivalent carbonyls in the catenane into a single peak, as found for the macrocycle, can still be achieved for the former but only at high scan rates and low temperatures, which freeze out the intrinsic dynamics of the mechanically interlocked molecule. At slower scan rates, however, the presence of irreversibility in the CV curve of the catenane shows that intramolecular reactions occur in the catenane that do not occur in the macrocycle. Quantum chemical calculations and the electrochemical behavior suggest that this intramolecular reaction is the soldering of the two macrocycles at the carbon atoms of the reduced carbonyls, leading to electrochemical braking of macrocyclic ring circumrotation. This could provide a useful means of switching “on” and “off” the dynamics of hydrogen bond-assembled interlocked architectures in material-based devices.

Acknowledgment. This work has been supported in part by the European Community: TMR contract no. FMRX-CT96-0059 and no. FMRX-CT97-0097, MURST and University of Bologna. F.Z. also acknowledges partial support from MURST project “Dispositivi Supramolecolari”.

References and Notes

(1) (a) Schill, G. *Catenanes, Rotaxanes and Knots*; Academic Press: New York, 1971. (b) Amabilino, D. B.; Stoddart, J. F. *Chem. Rev.* **1995**, *95*, 2725. (c) Sauvage, J.-P. *Acc. Chem. Res.* **1990**, *23*, 319. (d) Gibson, H. W.; Bheda, M. C.; Engen, P. T. *Prog. Polym. Sci.* **1994**, *19*, 843. For octaamide benzylic amide catenanes see: (e) Johnston, A. G.; Leigh, D. A.; Pritchard, R. J.; Deegan, M. D *Angew. Chem., Int. Ed. Engl*. **1995**, *34*, 1209. (f) Johnston, A. G.; Leigh, D. A.; Nezhat, L.; Smart, J. P.; Deegan, M. D *Angew. Chem., Int. Ed. Engl*. **1995**, *34*, 1212. For amphiphilic benzylic amide catenanes see: (g) Leigh, D. A.; Moody, K.; Smart, J. P.; Watson, K. J.; Slawin, A. M. Z. *Angew. Chem., Int. Ed. Engl*. **1996**, *35*, 306. For benzylic amide rotaxanes see: (h) Johnston, A. G.; Leigh, D. A.; Murphy, A.; Smart, J. P.; Deegan, M. D. *J. Am. Chem. Soc.* **1996**, *118*, 10662. (i) Leigh, D. A.; Murphy, A.; Smart, J. P.; Slawin, A. M. Z. *Angew. Chem., Int. Ed. Engl*. **1997,** *36*, 728. For a class of amide-based catenanes where the macrocyclic rings cannot circumrotate see: (j) Hunter, C. A. *J. Am. Chem. Soc.* **1992**, *114*, 5303, (k) Vögtle, F.; Dunnwald, T.; Schmidt, T. *Acc. Chem. Res.* **1996**, *29*, 451.

(2) For discussions of intercomponent motion in interlocked molecules see: (a) Anelli, P.-L.; Spencer, N.; Stoddart, J. F. *J. Am. Chem. Soc.* **1991**, *113*, 51313. (b) Ashton, P. R.; Bissell, R. A.; Spencer, N.; Stoddart, J. F.; Tolley, M. S. *Synlett* **1992**, 914. (c) Ashton, P. R.; Bissell, R. A.; Górski, R.; Philp, D.; Spencer, N.; Stoddart, J. F.; Tolley, M. S. *Synlett* **1992**, 919. (d) Ashton, P. R.; Bissell, R. A.; Spencer, N.; Stoddart, J. F.; Tolley, M. S. *Synlett* **1992**, 923. (e) Bissell, R. A.; Córdova, E.; Kaifer, A. E.; Stoddart, J. F. *Nature* **1994**, *369*, 133. (f) Benniston, A. C.; Harriman, A. *Angew. Chem., Int. Ed. Engl.* **1993**, *32*, 1459. (g) Benniston, A. C.; Harriman, A.; Lynch, V. M. *J. Am. Chem. Soc.* **1995**, *117*, 5275. (h) Benniston, A. C. *Chem. Soc. Rev.* **1996**, *25*, 427. (i) Ashton, P. R.; Ballardini, R.; Balzani, V.; Boyd, S. E.; Credi, A.; Gandolfi, M. T.; Gómez-López, M.; Iqbal, S.; Philp, D.; Preece, J. A.; Prodi, L.; Ricketts, H. G.; Stoddart, J. F.; Tolley, M. S.; Venturi, M.; White, A. J. P.; Williams, D. J. *Chem. Eur. J.* **1997**, *3*, 152. (j) Amabilino, D. B.; Sauvage, J.-P. *Chem. Commun.* **1996**, 2441. (k) Cárdenas, D. J.; Livoreil, A.; Sauvage, J.-P. *J. Am. Chem. Soc.* **1996**, *118*, 11980. (l) Baumann, F.; Livoreil, A.; Kaim, W.; Sauvage, J.-P. *Chem. Commun.* **1997**, 35. (m) Collin, J.-P.; Gavinã, P.; Sauvage, J.-P *Chem. Commun.* **1996**, 2005. (n) Lane, A. S.; Leigh, D. A.; Murphy, A. *J. Am. Chem. Soc.* **1997**, *119*, 11092. (o) Anelli, P.-L.; Asakawa, M.; Ashton, P. R.; Bissell, R. A.; Clavier, G.; Górski, R.; Kaifer, A. E.; Langford, S. J.; Mattersteig, G.; Menzer, S.; Philp, D.; Slawin, A. M. Z.; Spencer, N.; Stoddart, J. F.; Tolley, M. S.; Williams, D. J. *Chem. Eur. J.* **1997**, *3*, 1113−1135. (p) Murakami, H.; Kawabuchi, A.; Kotoo, K.; Kunitake, M.; Nakashima, N. *Chem. Eur. J.* **1997**, *119*, 7605−7606. (q) Gong, C.; Glass, T. E.; Gibson H. *Macromolecules* **1998**, *31*, 308−313.

(3) For catenanes where structure variations effect circumrotational dynamics see: (a) Anelli, P.-L.; Ashton, P. R.; Ballardini, R.; Balzani, V.; Delgado, M.; Gandolfi, M. T.; Goodnow, T. T.; Kaifer, A. E.; Philp, D.; Pietraszkiewicz, M.; Prodi, L.; Reddington, M. V.; Slawin, A. M. Z.; Spencer, N.; Stoddart, J. F.; Vicent, C.; Williams, D. J. *J. Am. Chem. Soc.* **1992**, *114*, 193. For catenanes where solvent variations effect circumrotational dynamics and translational isomerism see: (b) Ashton, P. R.; Ballardini, R.; Balzani, V.; Credi, A.; Gandolfi, M. T.; Menzer, S.; Pérez-García; Prodi, L.; Stoddart, J. F.; Venturi, M.; White, A. J. P.; Williams, D. J. *J. Am. Chem. Soc.* **1995**, *117*, 11171. For chemical, electrochemical and photochemical driven macrocyclic ring motions in catenanes see: (c) Livoreil, A.; Sauvage, J.-P.; Armaroli, N.; Balzani, V.; Flamigni, L.; Ventura, B. *J. Am. Chem. Soc.* **1997**, *119*, 12114. (d) Asakawa, M.; Ashton, P. R.; Balzani, V.; Credi, A.; Hamers, C.; Mattersteig, G.; Montalti, M.; Shipway, A. N.; Spencer, N.; Stoddart, J. F.; Tolley, M. S.; Venturi, M.; White, A. J. P.; Williams, D. J. *Angew. Chem., Int. Ed. Engl.* **1998**, *37*, 333.

(4) Vögtle et al. have recently reported an example where one ring can rotate about the other: Baumann, S.; Jäger, R.; Ahuis, F.; Kray, B.; Vögtle, F. *Liebigs Ann./Recueil* **1997**, 761.

(5) Leigh, D. A.; Murphy, A.; Smart, J. P.; Deleuze, M. S.; Zerbetto, F. *J. Am. Chem. Soc.* **1998**, *120*, 6458.

(6) (a) Ge, Y.; Lilienthal, R. R.; Smith, D. K. *J. Am. Chem. Soc.* **1996**, *118*, 3976. (b) Deans, R.; Niemz, A.; Breinlinger, E. C.; Rotello, V. M. *J. Am. Chem. Soc.* **1997**, *119*, 10863. For an excellent recent review of the electrochemistry of supramolecular and mechanically interlocked systems see: Boulas, P. L.; Gómez-Kaifer, M.; Echegoyen, L. *Angew. Chem., Int. Ed. Engl.* **1998**, *37*, 216.

(7) (a) Kuwana, T.; Bublitz, D. E.; Hoh, G. *J. Am. Chem. Soc.* **1960**, *82*, 5811. (b) Roffia, S.; Marcaccio, M.; Paradisi, C.; Paolucci, F.; Balzani, V.; Denti, G.; Serroni, S.; Campagna, S. *Inorg. Chem.* **1993**, *32*, 3003. (c) Paolucci, F.; Marcaccio, M.; Roffia, S.; Orlandi, G.; Zerbetto, F.; Prato, M.; Maggini, M.; Scorrano, G. *J. Am. Chem. Soc*. **1995**, *117*, 6572.

(8) Ceroni, P.; Paolucci, F.; Paradisi, C.; Juris, A.; Roffia, S.; Serroni, S.; Campagna, S.; Bard, A. J. *J. Am. Chem. Soc*. **1998**, *120*, 5480.

(9) Yee, E. L.; Cave, R. J.; Guyer, K. L.; Tyma, P. D.; Weaver, M. J. *J. Am. Chem. Soc.* **1979**, *101*, 1131.

(10) Amatore, C.; Lefrou, C.; Pfluger, F. *J. Electroanal. Chem.* **1989**, *270*, 43.

(11) Suzuki, H. *Electronic Absorption Spectra and Geometry of Organic Molecules*; Academic Press: New York, 1967.

(12) (a) Ammar, F.; Saveant, J. M. *J. Electroanal. Chem.* **1973**, *47*, 215. (b) Benson, S. W. *J. Am. Chem. Soc.* **1958**, *80*, 5151.

(13) Bard, A. J.; Faulkner, L. R. *Electrochemical Methods*; Wiley: New York, 1980; p 238.

(14) (a) Evans, D. H. In *Encyclopedia of Electrochemistry of the Elements (Organic Section)*; Bard, A. J., Lund, H., Eds.; Marcel Dekker: New York, 1978; Vol. 12, Chapter 1. (b) Kuroda, Y.; Seshino, H.; Kondo, T.; Shiba, M.; Ogoshi, H. *Tetrahedron Lett.* **1997**, *38*, 3939.

(15) The simulation of the electrochemical behavior of a multiparameter system, like the present catenane, is inherently limited: the determined rate constants are somewhat inaccurate, as the values obtained depend on the choice of standard potentials. As the kinetic shift will increase 30 mV/decade increase in rate constant, an error of 30 mV in the standard potential will give a 10-fold error in rate constant.

(16) (a) Stephens, P. W.; Bartel, G.; Fargel, G.; Tegze, M.; Janossy, A.; Pekker, S.; Oszlanyi, G.; Forro, L. *Nature* **1994**, *370*, 636. (b) Choi, C. H.; Kertasz, M. *Chem. Phys. Lett.* **1998**, *282*, 318. For a recent example of a long C−C bond: (c) Baldridge, K. K.; Kasahara, Y.; Ogawa, K.; Siegel, J. S.; Tanaka, K.; Toda, F. *J. Am. Chem. Soc.* **1998**, *120*, 6167.

(17) Morton, J. R.; Preston, K. F.; Kirnsic, P. J.; Hill, S. A.; Wasserman, E. *J. Am. Chem. Soc.* **1992**, *114*, 5454.